Available online at www.sciencedirect.com
ScienceDirect
Ceramics International 34 (2008) 189–195
CERAMICS INTERNATIONAL
www.elsevier.com/locate/ceramint

Non-destructive characterisation of alumina/aluminium titanate composites using a micromechanical model and ultrasonic determinations Part II. Evaluation of microcracking

M.G. Hernández [a], S. Bueno [b], T. Sánchez [a], J.J. Anaya [a], C. Baudín [b,*]

[a] *Instituto de Automática Industrial, CSIC, La Poveda, 28500 Arganda del Rey, Madrid, Spain*
[b] *Instituto de Cerámica y Vidrio, CSIC, Kelsen 5, 28049 Madrid, Spain*

Received 15 May 2006; received in revised form 26 June 2006; accepted 27 September 2006
Available online 7 November 2006

Abstract

A method for non-destructive detection of microcracks in ceramic composites is described. The method involves the combination of ultrasound characterisation with the application of a three-phase micromechanical model, which considers cracks and pores as void constituents. Four alumina-aluminium titanate materials with different levels of microcracking, from no cracks (monophase alumina) to severely cracked (alumina + 40 vol.% of aluminium titanate) including an alumina + 10 vol.% aluminium titanate material with incipient microcracking have been developed to test the validity of the method. Specimens have been fabricated by colloidal processing and the longitudinal and transverse ultrasound velocities have been determined by the ultrasonic pulse-echo and transmission ultrasound-immersion techniques, employing a digital signal processing. It has been demonstrated that it is possible to differentiate between pores and microcracks, both modelled as void constituents, in terms of the aspect ratio.

Keywords: B. Composites; D. Al_2O_3; D. Al_2TiO_5; Ultrasounds; Microstructure

1. Introduction

Alumina (Al_2O_3)/aluminium titanate (Al_2TiO_5) composites constitute a wide family of materials with high potential for structural applications. A strict control of the degree of microcracking during cooling is needed to optimise the mechanical behaviour of these composites as a function of the application. In this sense, it would be highly suitable the use of non-destructive methods to characterise the level of microcracking in alumina/aluminium titanate composites before use. In this work, the suitability of the use of a micromechanical model [1,2] together with ultrasonic determinations to evaluate the level of microcracking of alumina/aluminium titanate composites is evaluated. For the model to be applicable, the elastic constants of the solid constituents of the materials, alumina and aluminium titanate, have to be known. These constants have been previously determined in Part I of this work [2].

Non-Destructive Evaluation Techniques, NDE, such as ultrasonic techniques have long been used to obtain data about the presence of cracks in materials. The information contained in the ultrasonic signals can be analysed in terms of ultrasonic velocity, ultrasonic wave attenuation or structural noise. Out of these three possible approaches, the ultrasonic velocities have been selected in this work to evaluate the extent of microcracking. The methodology consists in the use of the existing relationships between the elastic properties and density of the materials and the ultrasonic velocities. The elastic properties are described as a function of the microstructural characteristics of the material, geometry, distribution and orientation of the constituent phases, by means of a micromechanical model [1,2]. Microcracks are modelled in the same way as porosity as ellipsoids; discrimination between these two microstructural characteristics is done on the basis of the aspect ratio.

* Corresponding author. Tel.: +34 91 735 58 40; fax: +34 91 735 58 43.
E-mail address: cbaudin@icv.csic.es (C. Baudín).

0272-8842/$32.00
doi:10.1016/j.ceramint.2006.09.007

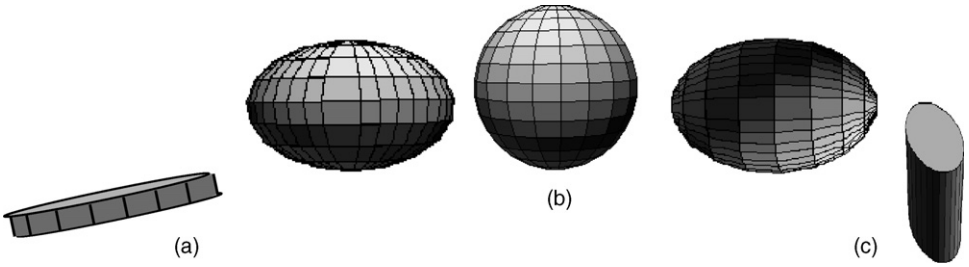

Fig. 1. Particular cases for the shapes of spheroids: (a) oblate, (b) sphere, and (c) prolate.

1.1. Micromechanical model

In the general expression of the micromechanical model that relates ultrasonic velocities and total density with the effective elastic properties of the matrix and the inclusions and the geometry of the inclusions described in Part I [2], the distribution, orientation and geometry of the inclusions is described by the Wu's tensor $\langle T^i \rangle$, ($i = p$, t, for porosity and aluminium titanate, respectively). The components of $\langle T^i \rangle$ in global coordinates can be calculated using the usual transformation of tensors, from $\left\langle T^{i'} \right\rangle$ [3]. The $T^{i'}$ tensor in local coordinates is given by:

$$\langle T^{i'} \rangle = [I + S(C^m)^{-1}(C^i - C^m)]^{-1} \quad (1)$$

where C^m and C^i are the elastic constants of the matrix and the inclusion, respectively, and S is the Eshelby's tensor that describes the inclusion geometry, in a general way, by an ellipsoid [4]. For an isotropic matrix, the tensor S depends only on the Poisson's ratio of the matrix and the aspect ratio, α, of the inclusions, defined as the relative size of the three axes of the inclusion a_1, a_2 and a_3.

For the sake of simplification, in this work the inclusions were modelled as spheroids, for which the aspect ratio is the relation between the size of the axis which is different and that of the two axes of the same size. For an oblate spheroid ($a_1 < a_2 = a_3$) the aspect ratio is $\alpha = a_1/a_3 < 1$; for a prolate spheroid ($a_1 > a_2 = a_3$), $\alpha = a_1/a_3 > 1$ and $\alpha = 1$ for the spherical inclusions. In Fig. 1 the particular cases of the geometry of the inclusions considered in this work, from disk shape ($\alpha \to 0$) to extended cylinders ($\alpha > 10$) are shown.

In this investigation, the alumina/aluminium titanate composites were modelled as constituted by three phases: the alumina matrix and two types of inclusions, aluminium titanate and voids (pores or microcracks). Porosity and microcracks were differentiated by their aspect ratio: $\alpha = 1$, for closed pores described as spheres, and $\alpha \to 0$ for microcracks, described as oblate spheroids.

1.2. Effect of the geometry of the inclusions on ultrasonic velocity

To evaluate theoretically the influence of the geometry of the voids on the ultrasonic velocities, homogeneous and isotropic composites of alumina with 40 vol.% of spherical aluminium titanate grains and volume fractions of voids varying between 0 and 30% were simulated. The elastic properties of alumina and aluminium titanate used were those determined in part I [2]. This influence is plotted for the longitudinal velocity in Fig. 2a. A decrease of velocity with the volume fraction of voids is observed. There is very little influence of the aspect ratio on velocity for large values of α, and a steep decrease occurs for ratios smaller than 0.5, which are closer to the geometry of microcracks.

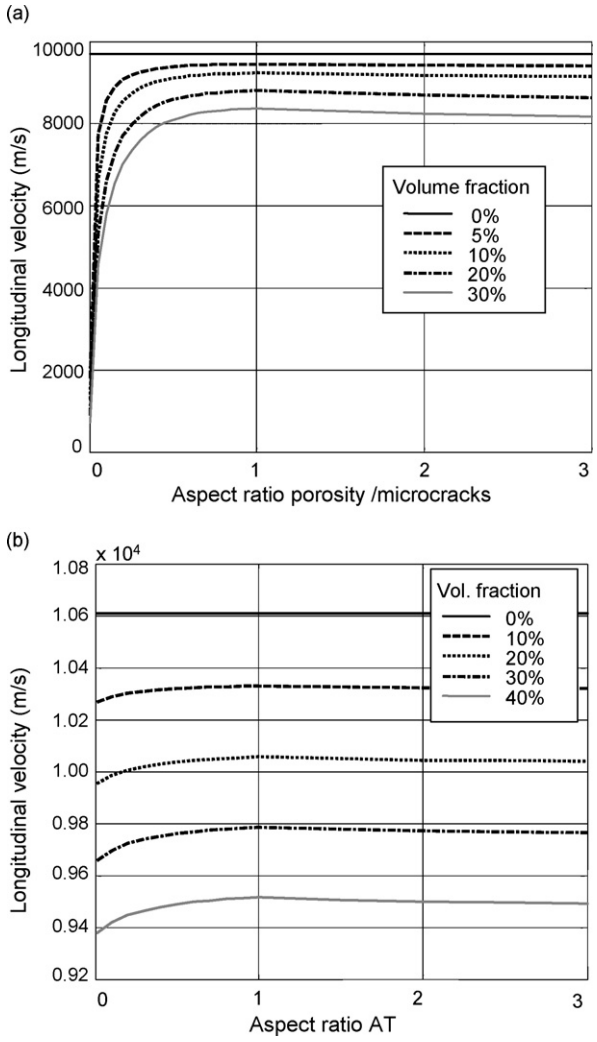

Fig. 2. Effect of geometry and volume fraction of the inclusions on the ultrasonic longitudinal velocity in alumina/aluminium titanate composites: (a) voids and (b) aluminium titanate.

To evaluate the effect of the geometry of the aluminium titanate grains on the ultrasonic velocity, porosity was kept constant (5 vol.%) and volume fractions of aluminium titanate varying between 0 and 40% were selected. As shown in Fig. 2b, there is a significant decrease of velocity with increasing aluminium titanate amounts. Conversely, there is very little effect of the aspect ratio, in particular, for α values close to or higher than 1.

2. Experimental

2.1. Material processing

One monophase alumina (Al_2O_3) and three alumina/aluminium titanate (Al_2TiO_5) composites were fabricated following the green processing procedure described in Part I [2]. For the composites, the starting powder mixtures were prepared as to get materials with 10 and 40 vol.% of aluminium titanate after reaction sintering. Two different thermal treatments were done, both with heating and cooling rates of 2 °C/min and with a dwell of 4 h at 1200 °C, with different high temperature treatments, at 1450 °C and 1550 °C during 2 and 3 h, respectively. The materials will be named A(1550), A-10AT(1550), A-40AT(1450) and A-40AT(1550) in order to describe composition and maximum sintering temperature.

For the ultrasonic determinations, the green compacts (70 mm × 70 mm × 12 mm) were cut into two pieces of equal dimensions before sintering and the sintered blocks were machined to get parallel surfaces (thickness ≅ 9.4 mm). Additional blocks were sintered as slip cast and machined after sintering into samples of 10 mm × 5 mm × 5 mm for thermal expansion determinations in a differential dilatometer (40 EP, Netzsch, Germany).

2.2. Microstructural characterisation

Densities of the sintered compacts were determined by Archimedes's method in water (European Standard EN

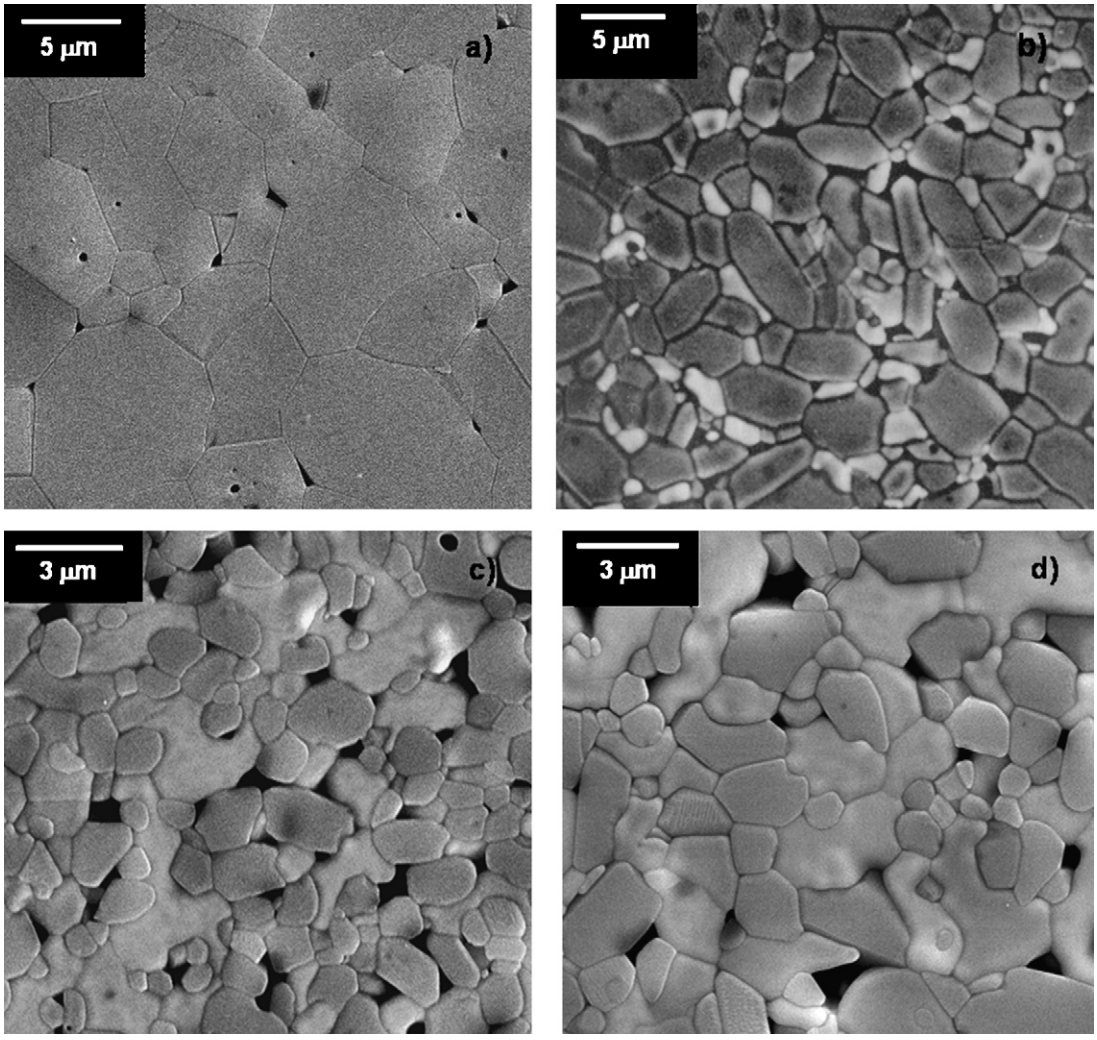

Fig. 3. Scanning electron micrographs of polished and thermally etched (20 °C below the sintering temperature, 2 min) surfaces of the studied materials. In the A-40AT materials some voids correspond to pull out of grains due to the difficult polishing of materials with high aluminium titanate contents. (a) A(1550) and (b) A-10AT(1550). Aluminium titanate grains (white), slightly elongated, are located mostly at grain boundaries and triple points in the alumina (grey) matrix. (c) A-40AT(1450), irregular shaped aluminium titanate grains are observed. (d) A-40AT(1550), irregular shaped aluminium titanate grains are observed.

1389:2003) and relative densities were calculated from the experimental values and the theoretical densities (3.99 g cm^{-3} for alumina, ASTM File 42-1468; and 3.70 g cm^{-3} for aluminium titanate, ASTM File 26-0040). Apparent open porosities were calculated from the difference between the mass of the dry specimens and the mass of the specimens soaked in water for 24 h after extracting the air from the recipient containing the samples using a vacuum pump.

Microstructural characterisation was performed by field emission scanning electron microscopy (FE-SEM, Hitachi, S-4700, Japan) on polished and chemically (HF 10 vol.%, 1 min) or thermally etched (20 °C below the sintering temperature during 1 min) surfaces.

2.3. Ultrasonic measurements

Ultrasonic velocities were determined by the pulse-echo method following the procedure described in Part I [2]. The two materials described above as well as specimens of the materials from Part I were characterised. In this case, not only the central parts of the samples but also the whole specimens were inspected, using inspection grids of 0.5 mm, in order to analyse the possibility of heterogeneously distributed microcracks. Each sample was inspected separately to be able to adapt the experimental conditions to its characteristics. The A(1550) and A-10AT(1550) specimens were inspected with a focused transducer at 20 MHz (Panametrics V317, 40 mm focal distance), doing an automatic scanning of each sample with a resolution of 0.5 mm, as in Part I. Due to the high attenuation that occurred in the A-40AT samples, it was necessary to use a transducer of smaller frequency than in the previous specimens (Krautkramer H5k, 5 MHz).

The ultrasonic pulse velocity, V_L, through the specimen was obtained from the time delay between two consecutive echoes $\Delta t = t_n - t_{n-1}$ and the thickness of the sample, s, by: $V_L = 2 \times s/\Delta t$. To minimise errors, the positions of two consecutive echoes were determined by digitally processing the gathered signals, to obtain the first crossing by zero.

3. Results

3.1. Microstructure and thermal expansion

The microstructures of the materials are presented in Fig. 3. Closed porosity was observed in all materials mostly located at grain boundaries and triple points. In the monophase alumina (Fig. 3a), additional small intragranular pores were observed. Aluminium titanate grains were slightly elongated in the A-10AT(1550) material (Fig. 3b) and had irregular shapes in both A-40AT composites (Fig. 3c and d). Microcracks were not observed in the monophase alumina, in agreement with the reversibility of the thermal expansion curve for this material, which was similar to those corresponding to the materials sintered at lower temperature studied in Part I (Fig. 4). Conversely, some small microcracks were observed in A-10AT(1550) which presented a slight thermal expansion hysteresis (Fig. 4b).

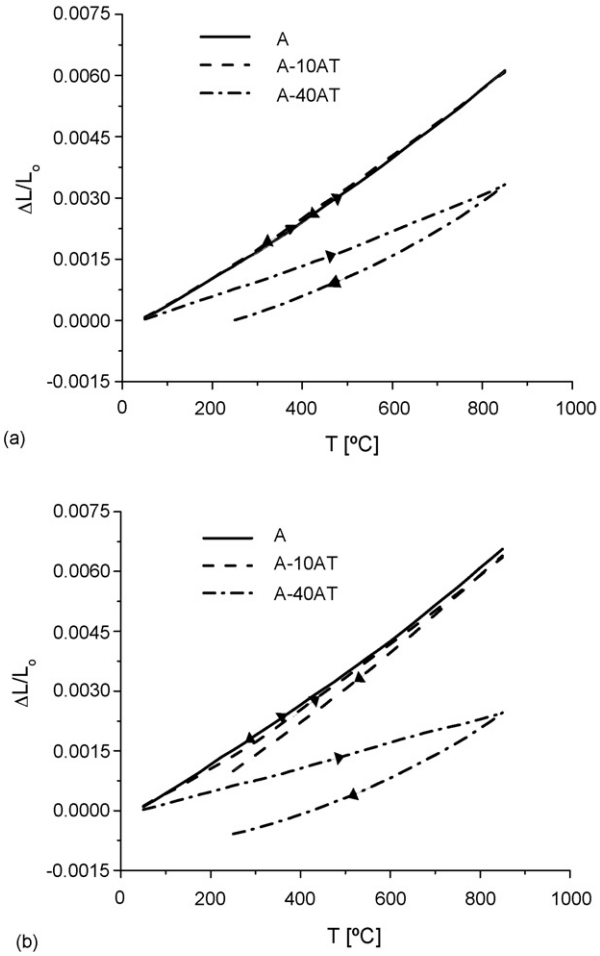

Fig. 4. Thermal expansion curves of the studied materials on heating and cooling at 5 °C/min. Reversibility is observed in monophase alumina. In alumina/aluminium titanate composites different degrees of hysteresis are observed. (a) Materials treated at 1450 °C, 2 h and (b) materials treated at 1550 °C, 3 h.

Both composites containing 40 vol.% of aluminium titanate had significant thermal expansion hysteresis (Fig. 4) in agreement with the significant number of cracks observed in the low magnification micrographs of polished and chemically etched surfaces (Fig. 5a and b). These cracks, with lengths between 150 and 200 μm, had maximum crack opening displacements of about 5 μm (Fig. 5c) ($\alpha \cong 0.03$).

There were not elongated pores, which would correspond to open porosity, in any of the microstructures observed. This is in agreement with the fact that in fine grained materials, such as the ones studied here, no open porosity is present after sintering at high temperature, when the initial sintering stage is finished. Therefore, the significant open porosity values (Table 1) found in both materials containing 40 vol.% of aluminium titanate cannot correspond to the actual volume of open porosity but to microcracks.

3.2. Ultrasonic measurements

The average ultrasonic velocities for the studied materials are listed in Tables 2 and 3. Values decreased for increasing

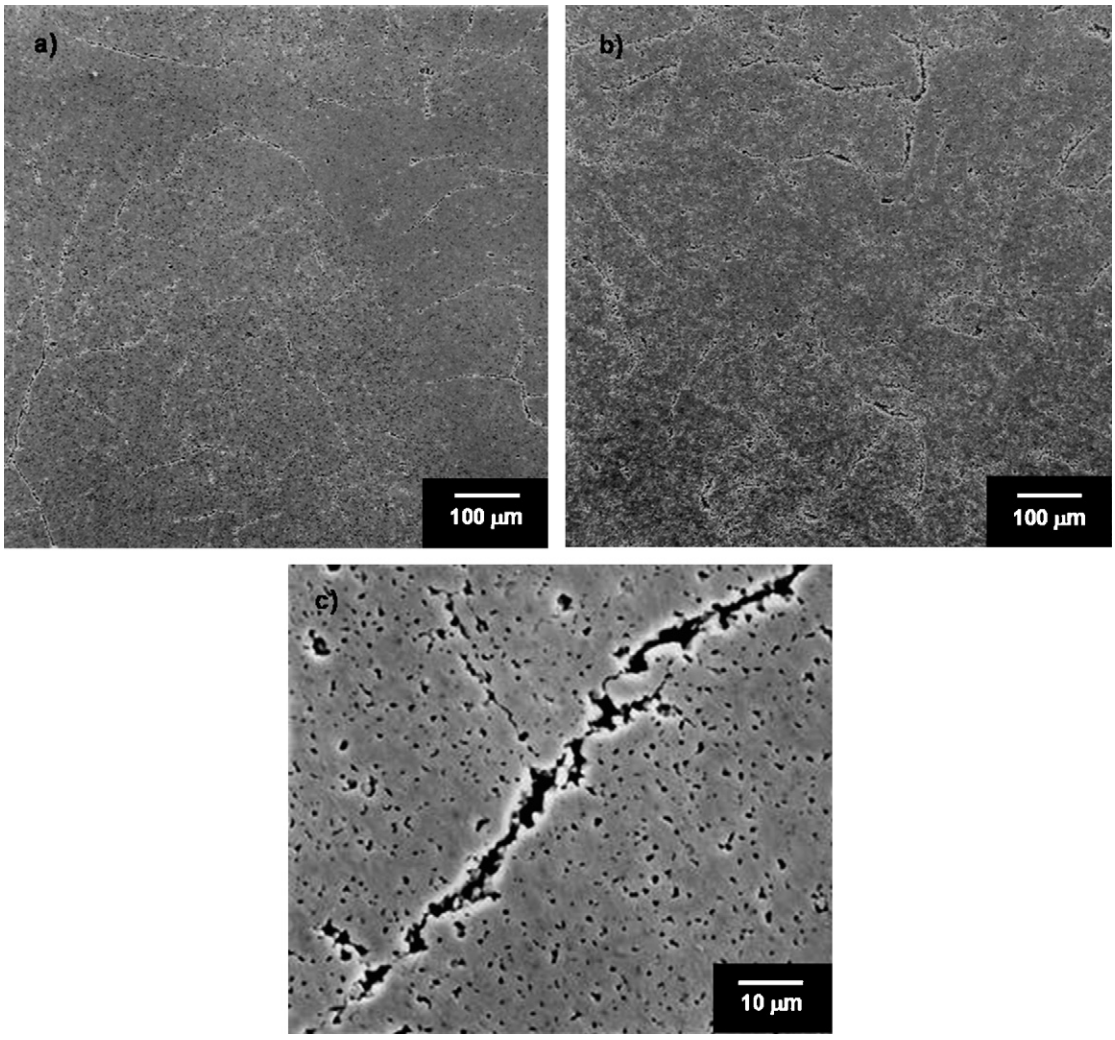

Fig. 5. Scanning electron micrographs of polished and chemically etched (HF 10 vol%, 1 min) surfaces showing the cracking of the A-40AT materials. (a) A-40AT(1450), (b) A-40AT(1550) and (c) detail of crack opening in the A-40AT(1450) material.

amounts of aluminium titanate, being this decrease extreme in the A-40AT materials, for which velocities one order of magnitude lower than those corresponding to the A-10AT specimens were determined. In addition, velocities decreased with the sintering temperature for specimens of the same composition, more in the A-40AT specimens (≅12%) than in the A (≅0.2%) and in the A-10AT (≅1%).

Table 1
Density and porosity of the studied materials

Material	$\rho_{relative}$ (g/cm^3)	Open porosity (%)	Total porosity (%)
A(1450)	3.90	0.0	2.3
A(1550)	3.89	0.0	2.4
A-10AT(1450)	3.88	0.1	2.1
A-10AT(1550)	3.88	0.2	2.0
A-40AT(1450)	3.55	4.4	8.4
A-40AT(1550)	3.56	3.9	8.0

Data for specimens from Part I, A(1450) and A-10AT(1450) are also included for comparison.

3.3. Application of the three-phase model

In order to evaluate whether the presence of microcracks in the material could be concluded from the ultrasonic velocities and the application of the model, the experimental values of velocity (Tables 2 and 3) were related to the values calculated using the micromechanical model for the experimental porosity values (Table 1) and different aspect ratios, from that for pores ($\alpha \cong 1$) to those corresponding to microcracks ($\alpha \to 0$).

As discussed in Part I [2], homogeneous and isotropic materials, have to be considered in order to simplify the three-phase model before application. This assumption is justified by the microstructural characteristics discussed above (Figs. 3 and 5) if the materials are considered in average. In addition, the following hypotheses regarding the properties of the materials were assumed:

(i) The elastic properties of alumina and aluminium titanate forming the solid constituents of the materials were taken as

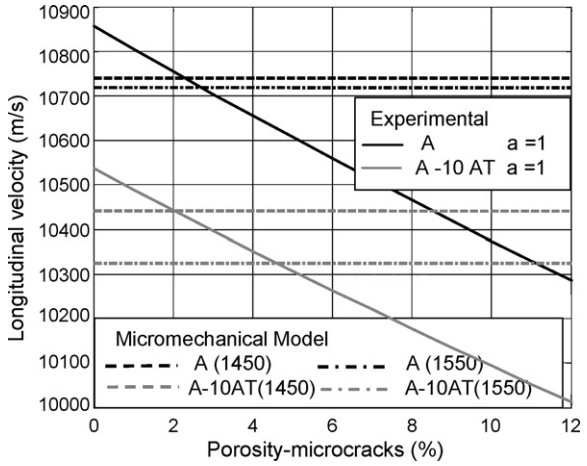

Fig. 6. Ultrasound velocity vs. the volume of pores in alumina and alumina/aluminium titanate (10 vol.%) materials according to the micromechanical model used (curves) together with the experimental values plotted as straight lines. For comparative purposes, values for the two materials developed in Part I are also plotted.

those of fully dense alumina and aluminium titanate evaluated in Part I and summarised in Table 4 [2].

(ii) The aluminium titanate grains were modelled as prolate spheroids with an aspect ratio of 1.4. This shape was selected as a compromise because it agreed well with that observed in the A-10AT(1550) specimens (Fig. 3b) and the aluminium titanate grains in materials A-40AT had very irregular shapes. Nevertheless, as seen in Fig. 2b, the aspect ratio of aluminium titanate has little influence on the ultrasonic velocity.

In Fig. 6 the theoretical relationships between the ultrasonic velocities and the porosity derived from the micromechanical model for the monophase alumina and the composites with 10 vol.% of aluminium titanate are plotted. Void inclusions in the shape of spheres $\alpha = 1$ were used to model porosity. A good agreement between the experimental values of velocity and the calculated ones for the porosity value of the materials (Table 1) is observed for A(1550) that, according with the microstructural observations and the thermal expansion behaviour, did not have microcracks. Conversely, the velocity predicted by the model is higher than the experimental one for the material that presented thermal expansion hystheresis (Fig. 4b), as a result of incipient microcracking, as discussed above.

Table 2
Predicted ($\alpha = 1$) and experimental (mean value and standard deviations) values of the ultrasonic longitudinal velocity for the studied A and A-A10 materials

Material	Experimental (m/s)	Predicted (m/s)
A(1450)	10740 ± 20	–
A(1550)	10719 ± 10	10,734
A-10AT(1450)	10442 ± 13	–
A-10AT(1550)	10324 ± 14	10,441

Table 3
Predicted and experimental (mean value and standard deviations) values of the ultrasonic longitudinal velocity for the studied A-40AT composites

Material	Experimental (m/s)	Predicted (m/s)			
		$\alpha = 1$	$\alpha = 0.1$	$\alpha = 0.01$	$\alpha = 0.001$
A-40AT(1450)	5106 ± 32	9340	8000	4050	1400
A-40AT(1550)	4479 ± 38	9360	8060	4130	1430

Table 4
Elastic properties, determined in Part I, and theoretical density of alumina and aluminium titanate

	E (GPa)	μ	C_{11}^m (GPa)	C_{44}^m (GPa)	ρ (g/cm^3)
Alumina	410.1	0.223	470.3	167.7	3.99
Aluminium titanate	154.9	0.329	228.7	58.3	3.70

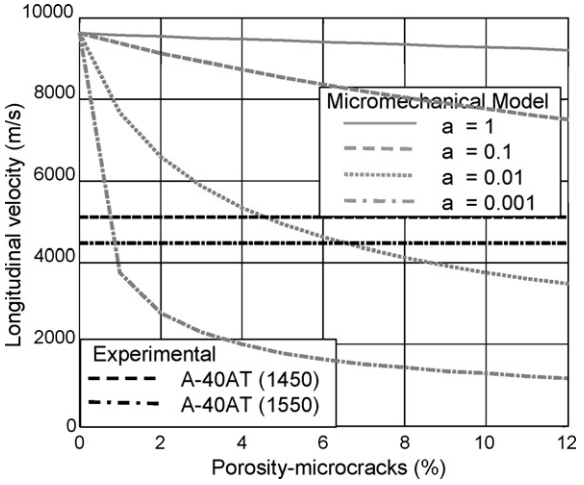

Fig. 7. Ultrasound velocity vs. the volume of pores in alumina and alumina/aluminium titanate (40 vol.%) materials according to the micromechanical model used (curves) together with the experimental values plotted as straight lines.

Fig. 7 and Table 3 show the results for the specimens with 40 vol.% of aluminium titanate. Four different aspect ratios were considered varying from spheres ($\alpha = 1$) to oblate spheroids ($\alpha = 0.001$). The best agreement of the experimental velocity values with those calculated for the total porosity levels of the materials (≅8 vol.%, Table 1) that resulted from microcracking, occurred for low aspect ratios ($\alpha \cong 0.01$). Therefore, the presence of the microcracks in the studied composites can be detected using non-destructive techniques such as the ultrasonic one proposed here by determining the aspect ratio that better describes the porosity of the materials in the micromechanical model.

4. Conclusions

A methodology for non-destructive evaluation of the presence of microcracks in ceramics composites has been proposed. The application of a micromechanical model of three phases to relate the ultrasonic velocity to microstructural

parameters allows discriminating between pores and microcracks, modelled as void constituents, in the material in terms of the aspect ratio.

Acknowledgements

The financial support of Spanish Ministry of Science and Technology (Project DPI 2003-08628-C03-00) and the Projects CICYT MAT2003-00836 and CAM GRMAT0707-2004 is acknowledged. M.G. Hernández is supported by a postdoctoral CSIC-I3P contract granted by the European Social Fund. S. Bueno acknowledges the financial support of the Grant CSIC I3P-BPD2001-1 (Spain).

References

[1] M.G. Hernández, J.J. Anaya, L.G. Ullate, A. Ibañez, Formulation of a new micromechanic model of three phases for ultrasonic characterization of cement-based materials, Cement Concrete Res. 36 (2006) 617–624.
[2] S. Bueno, M.G. Hernández, T. Sánchez, J.J. Anaya, C. Baudín, Non-destructive characterisation of alumina/aluminium titanate composites using a micromechanical model and ultrasonic determinations. Part I. Evaluation of the effective elastic constants of aluminium titanate, Ceramics International 34 (2008) 181–188.
[3] T.T. Wu, The effect on inclusion shape on the elastic moduli of a two phase material, Int. J. Solids Struc. 2 (1966) 1–8.
[4] J.D. Eshelby, The determination of the elastic field of an ellipsoidal inclusion and related problems., Proc. Royal Soc. London A241 (1957) 376–396.